Theory, Techniques and Validation of Over-the-Air Test Methods for Evaluating the Performance of MIMO User Equipment

Application Note

Abstract

Several over-the-air (OTA) test methods have been proposed to characterize the radiated performance of multiple input multiple output (MIMO) devices. Knowing that antenna gain and spatial correlation are important factors to system performance, it has become necessary to include OTA testing of MIMO antenna performance. This paper will discuss three predominant OTA test methods including the two-stage OTA method, the multiple test probe OTA method and the reverberation chamber method. In some test configurations, the probe antennas are connected to a wireless channel emulator, such as the Agilent N5106A PXB, to emulate real-world multipath environments. In addition, this paper will discuss two types of MIMO channel models, the correlation-based and geometry-based models, and show how antenna and spatial characteristics at the MIMO transmitter and receiver can be separated into independent terms. Separating antenna gains and spatial characteristics allow the practical implementation of accurate OTA measurement systems using commercially available test instrumentation. This paper will also show measurements of spatial correlation and system capacity taken from commercial MIMO devices, and comparisons will be made using several OTA methods. It is assumed that the reader is familiar with basic concepts of MIMO technologies and additional background can be found in the References section [1], [2], [3]. Additional information on the 3GPP MIMO channel models can also be found in References [4].

Agilent Technologies

Introduction

Traditional conducted test methods for testing the performance of single input single output (SISO) devices is typically achieved with a system comprised of a base station (BS) signal generator and a wireless channel emulator directly cabled to the device under test (DUT). The channel emulator typically provides a selection of channel models that faithfully reproduce a wireless signal propagation environment based on time-domain fading, Doppler spreading and path loss of the BTS signals. These test systems are ideally suited for characterizing the SISO mobile subscriber (MS) or user equipment (UE) under controlled and repeatable conditions without the antenna's influence. Many test specifications, including 3GPP TS 34.114 [5], also require OTA testing of SISO devices in order to include antenna effects during the measurements. SISO OTA testing performed in an anechoic chamber actively measures the total radiated power (TRP) and total radiated sensitivity (TRS) [6] of the UE. The SISO test is mainly used to test the antenna gain and the sensitivity of the receiver due to antenna gain and UE self interference. The SISO test does not require a fading channel. It is known that this type of testing is not sufficient for characterizing the performance of MIMO UE, and OTA testing of MIMO antenna systems must include a model of the spatial correlation effects between antenna elements and interaction with the surrounding multipath environment. While the basic measurement equipment used in SISO OTA test systems can also be included in a MIMO OTA test system, additional equipment measurement techniques and improved channel models will be required to accurately represent the spatial characteristics of the multipath and the MIMO antenna characteristics.

In any wireless system, a signal propagating through a terrestrial channel can arrive at the destination along a number of different paths, referred to as multipath. Each path can be associated with a time delay and a set of spatial angles, one angle at the transmitter and one at the receiver. For example, Figure 1a shows a simplified diagram of a 2x2 MIMO system operating in a multipath environment. Between the Tx1 and Rx0 antenna pair, the figure shows a direct line-of-sight (LOS) path and several other non-LOS (NLOS) paths. Each transmit and receive antenna pair would ideally have an uncorrelated set of multipath characteristics depending on the antenna spacing and polarizations. The multipath characteristics arise from scattering, reflection and diffraction of the radiated energy by objects in the surrounding environment. The various propagation mechanisms influence the channel's spatial characteristics, signal fading, Doppler and path loss. At each receive antenna, multipath propagation results in both a time spreading, referred to as delay spread, and spatial spreading as transmitted signals follow unique transmission paths from the BS to the UE antennas arriving at different angles with different path losses. At the receive antenna, each path can be associated with an angle of arrival (AoA) as measured relative to the array normal. These signal paths are also associated with an angle of departure (AoD) as the transmitted signals leave the BS antenna and enter the channel. The AoDs are measured relative to the normal of the transmit antenna array. The spatial characteristics of the wireless channel are modeled using a spatial distribution referred to as power angle spectrum (PAS). As MIMO performance is strongly influenced by spatial correlation introduced by the PAS and antenna characteristics, it is extremely important to measure MIMO devices using an OTA test system that can accurately emulate realistic channels and include the effects of angular spread, direction of arrival, antenna gain, antenna spacing and antenna polarization. For example, as shown in Figure 1b, the antenna patterns for Rx0 and Rx1 exhibit peak gains separated by 180 degrees. The difference between antenna patterns as a function of angle may help to de-correlate the signals arriving at each receive antenna, therefore it is important to include the antenna characteristics in any MIMO channel model and associated OTA test system in order to get an accurate measurement of the MIMO UE performance.

As in all test systems, a balance must be achieved between the accuracy of the MIMO OTA measurement approach and the speed and complexity of the overall test system. It may also be beneficial that the MIMO OTA test system support backward compatibility to SISO operation. Three predominant OTA test methods examined in this application note include the two-stage OTA method, the multiple test probe method and the reverberation chamber method. The goal of this application note is to introduce the test requirements, channel models available for OTA testing, equipment configuration and OTA chamber requirements. Also included are the channel model implementation measurements and validation using the different OTA test methods. The next section begins with an introduction of the desired figures of merit (FOM) measured in order to determine a "good" MIMO device from a "bad" device.


(a) 2x2 MIMO system   (b) Antenna gain patterns
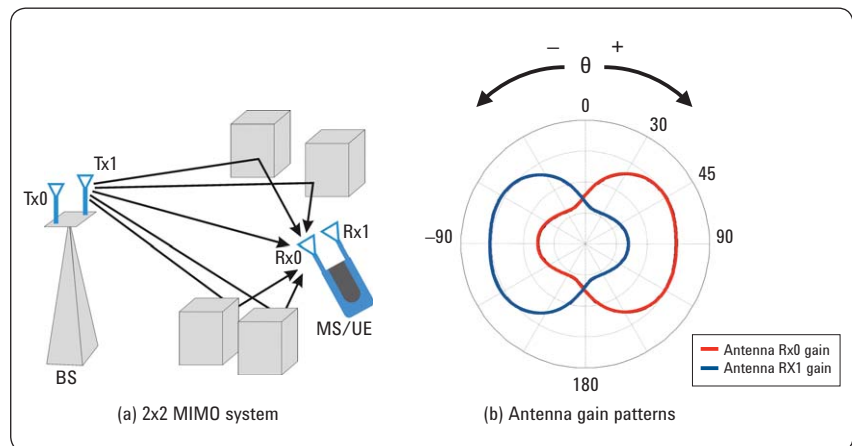
Figure 1. (a) Diagram of a simple wireless 2x2 MIMO configuration and (b) associated antenna gain pattern for the two MS/UE antennas.

MIMO Figures of Merit

Traditionally, the performance of 2G and 3G systems, such as those with SISO configurations, are assessed with specified test parameters or figures of merit (FOMs). These FOMs include maximum transmit power and receive sensitivity and end-to-end system bit error rate (BER) or frame error rate (FER). These measurements can be performed with test equipment cabled directly to the UE or can be over-the-air to include the effects of antenna radiation and antenna interaction with the UE. With the introduction of MIMO, the antenna design and associated gain pattern become fundamental to the performance of the MIMO system as multipath and low correlation between multiple antennas provide the potential capacity increase over traditional SISO techniques.

The proposed list of FOMs for MIMO OTA testing, as defined by 3GPP, is shown in Table 1[6]. The FOMs include OTA and antenna radiation test parameters for measuring the performance of the UE in realistic environments. The FOMs are categorized as "active" and "passive" testing. Active device testing includes OTA measurements with an active transmitter. The transmitted signal is typically delivered by a BS signal emulator such as the Agilent E6621 wireless test set. Active testing may or may not include the emulation of multipath signal fading. Passive testing includes characterization of the MIMO antenna radiation. These measurements can be taken directly on the MIMO antenna array or from the UE when the equalizer response signal is available for characterizing the individual antenna element performance of the MIMO array. Passive testing does not require an active BS emulator or channel fading emulator. Passive antenna characterization may also include the use of a specific anthropomorphic mannequin (SAM) phantom head to measure the proximity effects between the human head model and the MIMO UE antenna array.

The predominant FOM for characterizing MIMO UE performance is MIMO throughput. This active end-to-end throughput measurement attempts to emulate a realistic user experience by testing the data capacity under the influence of signal fading and in a modeled environment with spatial variation. Organizations, such as the 3GPP, COST 2100 and CTIA develop standardized channel models that include the effects of path loss, shadow fading, delay spread, power delay profile (PDP), PAS, AoD, AoA and angle spread or azimuth spread (AS) in a variety of wireless environments including urban and suburban types. Modeling and emulating the spatial variations, including PAS and AS, and their effect on MIMO throughput will be discussed in more detail later in this application note.

Additional active FOMs include the TRP, TRS, channel quality indicator (CQI), and block error rate (BLER). The TRP and TRS performance metrics verify the peak throughput as well as cell edge performance. The TRP and TRS are measured without channel fading. The TRP is a measure of how much power the UE radiates and is defined as the integral of the power transmitted over the entire radiation sphere. The TRS is related to the power available at the antenna output such that a receive sensitivity threshold is achieved for each antenna polarization. Characterizing the performance of MIMO antennas is predominately performed using passive testing. Passive testing evaluates antenna efficiency, mean effective gain (MEG), antenna gain imbalance, spatial correlation and MIMO capacity. These passive FOMs are calculated using measured spatial antenna patterns obtained from traditional anechoic chamber test methods. For example, the MIMO capacity can be estimated using the measured antenna patterns and the selected multipath channel model. Together these parameters are used to calculate the ideal channel coefficients and related capacity based solely on the spatial properties without including the effects of DSP and baseband processing in the UE. Although passive measurement methods alone cannot directly provide the total end-to-end OTA performance of the UE, combining these separate passive measurements with a MIMO channel emulator can quickly yield similar results achievable by other more complex OTA test systems.

Table 1. List of FOMs for MIMO OTA measurement

Category	I	II	III	IV	V
FOMs	MIMO throughput (VRC)	TRP TRS	CQI BLER (FRC) MIMO throughput (FRC)	Antenna efficiency MEG	Gain imbalance Spatial correlation MIMO capacity
Requirements	MIMO T-put > X Mbps	TRP > +X dBm TRS < –X dBm	CQI > X BLER < X % T-put > X Mbps	Efficiency > –X dB MEG > –X dBi	Imbalance < X dB Correlation < X Capacity > X bps/Hz
Subject	OTA	OTA	OTA	MIMO antennas	MIMO antennas
Methodology	Active (with fading)	Active	Active (with fading)	Passive/Active	Passive

Modeling the Spatial Characteristics of the Multipath Channel

The multiplexing capacity gains achievable by using multiple antennas at both the transmitter (Tx) and the receiver (Rx) have generated so much interest in recent years that most modern wireless communication systems have options for MIMO implementations including the 802.11n WLAN, 802.16 WiMAX and 3GPP LTE. The capacity increase is obtained by the potential de-correlation between the channel coefficients introduced by the rich multipath environment establishing several parallel subchannels between the transmit antenna array and receive array [7]. However, system capacity is greatly reduced once the subchannels become highly correlated to the point where fully correlated subchannels result in a capacity degradation to that of a single subchannel as found in a SISO system. Traditional methods for modeling wireless channels, such as power delay profile (PDP) and Doppler spectrum, can accurately represent the multipath effects in a SISO system, but improved channel models are required for MIMO systems. The shortcoming of traditional models is that they typically do not include spatial effects introduced by antenna gain, antenna position, antenna polarization and UE movement within the multipath environment. To accurately model and test the performance of a MIMO UE, it is necessary to include the spatial characteristics of the environment and the antenna arrays.

When developing simulation and test strategies for characterizing the performance of the MIMO UE under realistic channel conditions, it becomes important to develop channel models that accurately emulate a spatially rich multipath environment. These spatial models, including correlation effects, can be implemented in their exact form or approximated within the system simulation or target test system. There are two basic types of channel models currently being studied for LTE OTA testing.

The first model uses a stochastic or correlation-based channel model of the multipath environment. This correlation-based model is a good fit for the two-stage OTA method which combines the spatial properties of the multipath with the spatial properties of the BS and UE antenna arrays. The second method is a geometry-based channel model, such as the spatial channel model (SCM) [4], that uses ray-tracing techniques approximate the multipath environment. The SCM technique is a good fit to the multiple test probe OTA test method, where the SCM is emulated with multiple probe antennas positioned within a large anechoic chamber. The accuracy in the SCM approximation is directly related to the number of test probes implemented in the OTA test system. The geometry-based SCM can also be implemented in the two-stage OTA test method with a large reduction in system complexity.

Correlation-based channel model

A simplified multipath channel within a 2x2 MIMO system is shown in Figure 2. In this case, the base station uses a two-element array for transmitting two data streams from the Tx0 and Tx1 antennas. The BS antenna array boresight is defined normal to the array and will be used as the reference point for determining the AoD from this array. In this example, the UE also contains two antenna elements and, similarly, its array boresight is defined as normal to the UE array and will be used as a reference for determining the AoA. The UE can also be moving relative to the BS with velocity (v) as shown in Figure 2.

The multipath environment in this example contains two groupings of multiple reflections or scatterers called clusters. A cluster is associated with a tight grouping of spatial angles around the BS and/or UE. The cluster can be representative of a large building with high architectural detail creating radio wave scattering from around the structure. Rather than attempt to include each reflected signal path and its associated AoD and AoA in the channel model, a statistical model can be created that includes the mean AoD and mean AoA for each cluster as well as an associated AS representing the distribution of angular power about each mean.

Cluster n in Figure 2 shows transmission path n connecting the BS array to the UE array. Path n leaving the BS has a mean AoD of $\theta_{n,AoD}$, and an AS of $\sigma_{n,AoD}$. At the UE, this path has an AoA of $\theta_{n,AoA}$, and an AS of $\sigma_{n,AoA}$. A typical BS would have a narrow AS due to the fact that the BS antenna array is located at a high elevation and away from most scatterers. In contrast, the UE is located at low elevation near a large number of local scatterers, resulting in a wide AS.
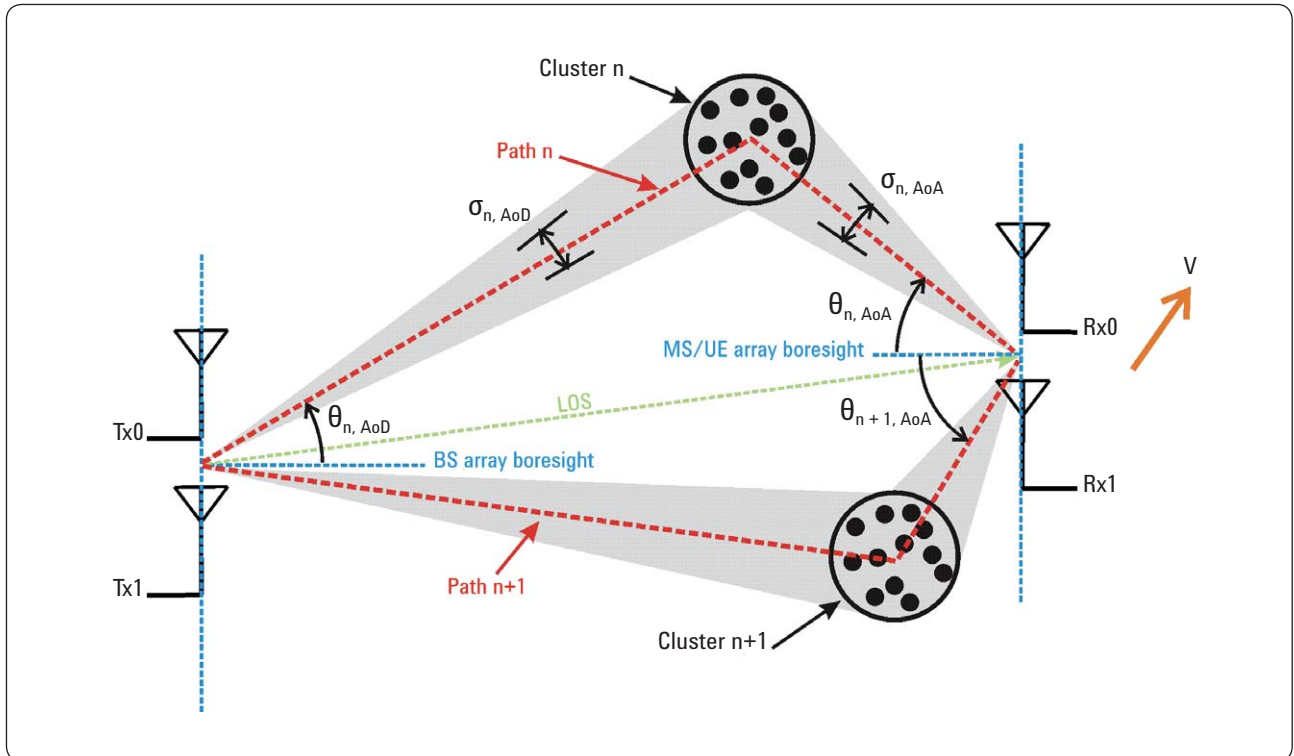

Figure 2. MIMO system showing an antenna array at both the BS and UE. Multipath reflections and/or scatterers are grouped into individual clusters and modeled as a single path with an associated angular spread.

The distribution of the signal power as a function of angle for each cluster can be characterized with a probability density function (PDF) [3]. The PDF is modeled using a Laplacian, Gaussian or uniform distribution. The distribution is selected based on the type of multipath channel to be modeled. For example, the spatial power distribution for an outdoor urban environment will often be modeled using a Laplacian distribution. The standard deviation of the PDF is the angular spread (AS), sometimes referred to as azimuth spread and usually defined in the horizontal or azimuth plane. The array PAS is a combination of PDFs from all the associated clusters, and is displayed as the average power at the antenna as a function of angle. This total angular power, integrated over 360 degrees in azimuth, is normalized to a value of one. Figure 3a shows a simulated PAS at the receive antenna array for a multipath channel having two large clusters, n and n+1, similar to the configuration shown in Figure 2. The PAS contains two distinctive peaks arriving at angles $\theta_{n,AoA}$ and $\theta_{n+1,AoA}$. These angles are relative to the antenna array boresight. A similar-looking PAS is found at the transmit antenna array for the associated departure angles. For this channel, the receive array PAS is best modeled using a truncated Laplacian PDF as shown in Figure 3b [3]. The mean AoAs for the modeled PDF coincide with the cluster peaks of the original PAS. The standard deviations, $\sigma_{n,AoA}$ and $\sigma_{n+1,AoA}$, can be independently optimized for each cluster. In theory, each antenna element in the receive array would have a slightly different PAS, but, in practice, especially for outdoor channels, the clusters are positioned relatively far from the array, making the AoAs approximately equal, so the same PAS can be assigned to each antenna element. The elements in the transmit array will also be assigned the same PAS, though the PAS distributions are usually quite different at the transmitter and receiver arrays. A more complex model would be required for a MIMO system having cross-polarized antenna elements. In this case, a different PAS may be required for each element in the cross-polarized antenna array. The PAS using truncated PDFs will be included in the correlation-based channel model and implemented as one option in the two-stage OTA test system.
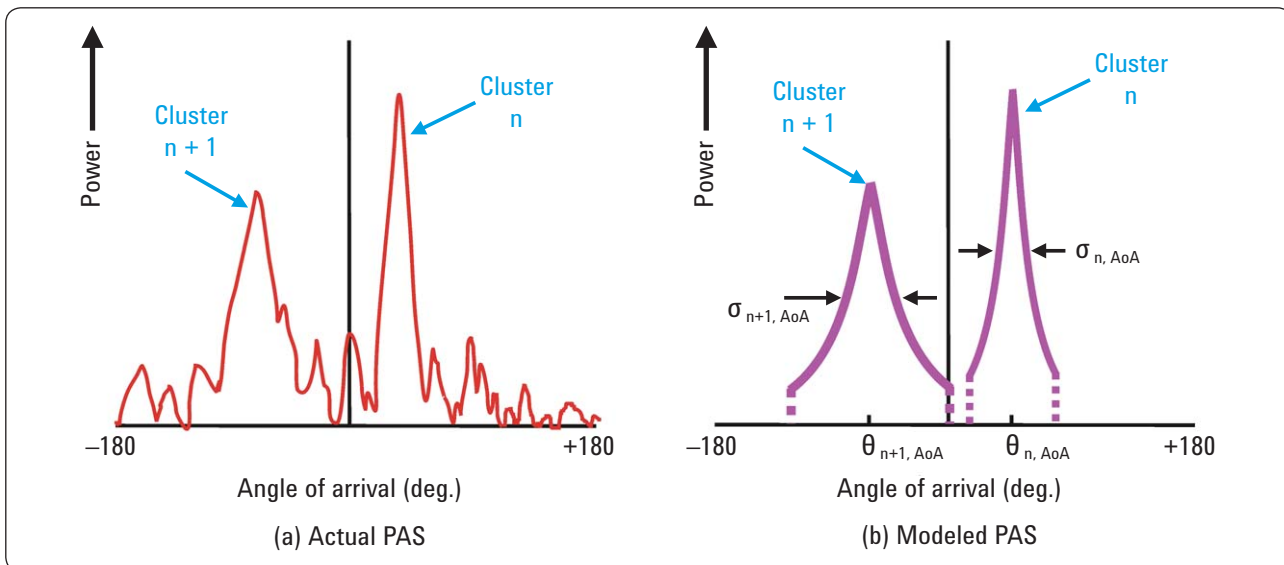

Figure 3. (a) PAS at the receive antenna array for a multipath channel having two clusters (b) equivalent PAS model using the truncated Laplacian PDF.

Geometry-based channel model using sum-of-sinusoids technique

An approximate model to the previously discussed angular distributions can be developed using sub-paths to produce the desired power spectrum associated with each cluster [8]. The proposed model is based on the sum-of-sinusoids technique that uses a set of sub-paths with predefined angular spacing and equal power level to produce the desired PDF distribution. Figure 4 shows an approximation to a Laplacian distribution using 20 equal-amplitude sub-paths. By approximating the distribution with a large number of sub-paths, a Rayleigh fading statistic can also be achieved as a function of time. Maintaining equal power for each sub-path will prevent any single sub-path from dominating the distribution and thereby producing Rician fading. There is a tighter grouping of sub-paths near the peak of the Laplacian distribution to place more power at the center of the distribution. The angular spacings are optimized to achieve a desired standard deviation or angular spread (AS). As the required AS widens, the sub-paths spread out further in angle and begin to approach a uniform distribution where the sub-paths are all equally spaced in angle. This sum-of-sinusoids model can be defined with even or odd number of sub-paths approximating the desired PAS distribution. Reference [8] has a procedure for calculating the appropriate angles for each sub-path.

The sub-path model, implemented as a geometry-based model in an OTA test system, will include a set of unique rays connecting the transmit and receive antennas. Figure 5 shows a simplified geometry-based model using a distribution of sub-paths to approximate a Laplacian PAS at the transmit antenna array and an associated grouping of sub-paths to model a Laplacian PAS at the receive antenna array. Figure 5 is simplified for clarity by showing only a single cluster, n, and five sub-paths connecting transmit antenna array to receive antenna array. For the simplified case, the mean AoD for transmit antenna array is θ_{AoD} and the mean AoA for receive antenna array is θ_{AoA}. The sub-path angular distributions are referenced to these AoD and AoA values.
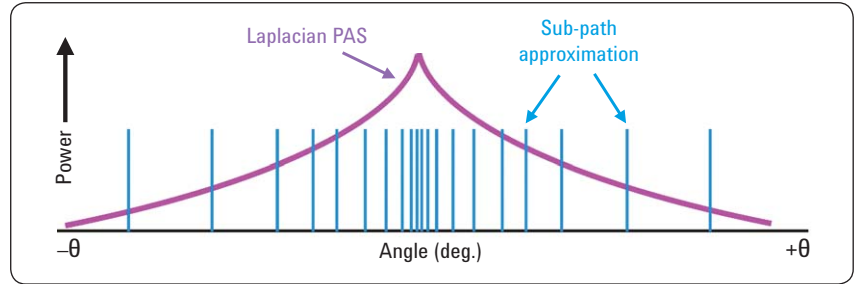

Figure 4. Approximation of a Laplacian PAS using 20 equal-amplitude sub-paths.
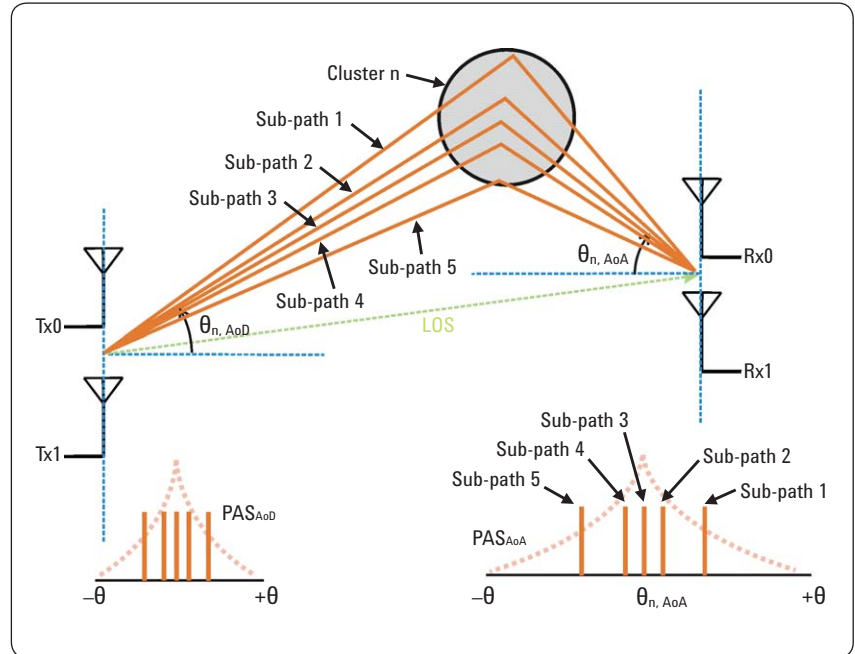
Figure 5. Geometry-based representation of the Tx PAS and Rx PAS using five sub-paths relating to cluster n.

The 3GPP has developed a technical specification for modeling the spatial characteristics of MIMO channels based on this ray-tracing or geometry-based approach. The model is defined as the SCM [4]. The SCM provides mathematical channel models for use in link-level and system level simulations of outdoor environments. This simulation model emulates small scale fading including effects of shadowing, path loss and inter-cell interference. The basic model defines three types of multipath environments namely the suburban macro, urban macro and urban micro. These models can be used with any antenna array configuration in order to simulate the MIMO system performance. All the SCM models assume a multipath channel with six clusters, defined by their mean AoD and AoA, with each cluster comprised of 20 equal-powered sub-paths used to approximate the associated PAS distribution.

Depending on the type of environment, the 3GPP SCM specifies PAS distributions for Laplacian and uniform PDFs. PAS distributions are modeled in the horizontal, or azimuth, plane as most outdoor scenarios typically experience little change in elevation characteristics. The SCM defines unique PAS distributions for all three multipath environments with individual sub-paths having a specified angular spread relative to the cluster's mean AoD and AoA. For example, Table 2 shows the relative angular positions for the 20 sub-paths required to model a single path having a 5 degree AS at the BS and a 35 degree AS at the UE operating within an urban microcell environment.

As defined in the 3GPP SCM, the angular spread for individual paths are fixed during simulations, but the AoDs, AoAs and time delays for each path are random variables for each iteration. The SCM procedure requires numerous iterations, or drops, to provide a statistical average of the MIMO performance. During a drop, which may cover several frames of a MIMO transmission, the spatial and delay characteristics remain fixed but the channel coefficients may undergo fast fading due to any relative motion of the UE. In this case, the channel coefficients are modified due to changing phase characteristics for each sub-path in the simulation. Additional information regarding the SCM environmental parameters for the SCM drop are provided in reference 3GPP TR 25.996 [4]. The 3GPP SCM will be the basis for OTA testing. As discussed in the next section, when using a reduced number of sub-paths, Rayleigh fading is not fully developed and, as a result, the power in each sub-path will require a separate process to introduce time fading. For example, a channel fader, such as the Agilent N5106A PXB, will be required to introduce Rayleigh fading to each sub-path.

Table 2. PAS sub-path AoD and AoA angular offsets for an urban micro environment [4]

Sub-path # (m)	Angular offset for a 5-deg AS at BS (degrees)	Angular offset for a 35-deg AS at UE (degrees)
1, 2	±0.2236	±1.5649
3, 4	±0.7064	±4.9447
5, 6	±1.2461	±8.7224
7, 8	±1.8578	±13.0045
9, 10	±2.5642	±17.9492
11, 12	±3.3986	±23.7899
13, 14	±4.4220	±30.9538
15, 16	±5.7403	±40.1824
17, 18	±7.5974	±53.1816
19, 20	±10.7753	±75.4274

Geometry-based channel model using quantized PAS

In many cases, when implementing an OTA test system using geometry-based channel models such as the 3GPP SCM, it may not be practical to include a large number of sub-paths in the sum-of-sinusoids technique. Unfortunately, reducing the number of sub-paths may not only reduce the accuracy of the PAS approximation but also has a secondary effect of altering the Rayleigh fading statistics in time. As previously discussed, the sum-of-sinusoids technique produces both the proper angular distribution as well as Rayleigh fading in time when the number of sub-paths is large. Greatly reducing the number of sub-paths in an OTA test system will require additional techniques to properly create Rayleigh fading.

Assuming that time fading will be introduced to each sub-path by other means, an alternate approximation to the PAS distribution can be made using a smaller number of sub-paths that effectively quantize the PAS amplitude and angular distribution. For example, Figure 6 shows the desired Laplacian PAS distribution and a quantized representation using three sub-paths with unequal amplitudes. The angular placement of the sub-paths and their associated amplitudes must be optimized to properly model the PAS distribution and fading characteristics when these three signals are combined at the receive antenna. Not shown in Figure 6, is the requirement that each sub-path be independently faded as a function of time in order to properly emulate the multipath channel. As described later in this application note, a channel emulator such as the Agilent N5106A PXB can be used to introduce sub-path fading in the OTA test system.
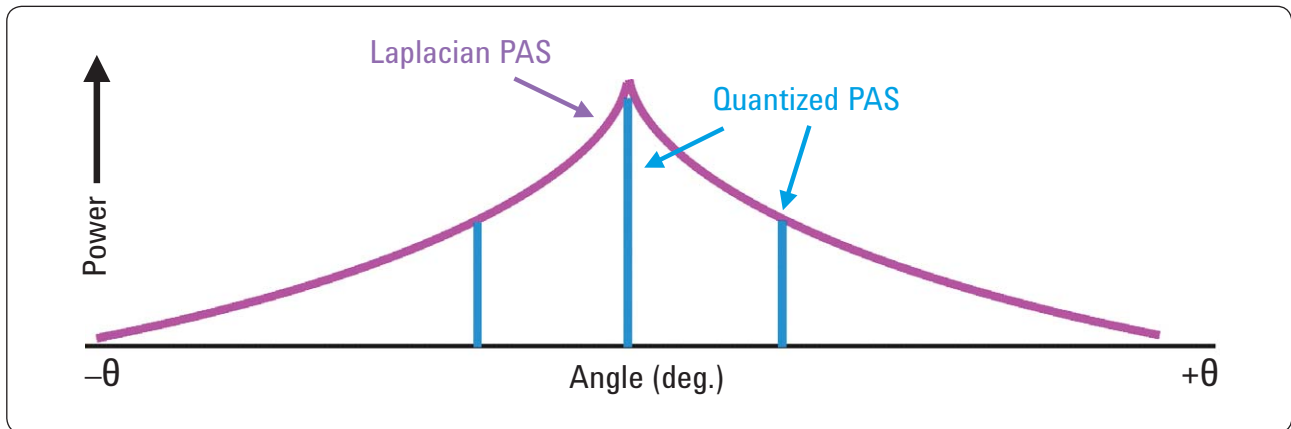

Figure 6. Quantized approximation of a Laplacian PAS using three unequal powered sub-paths.

Spatial Correlation Effects on MIMO Capacity

As mentioned previously, the capacity increase in a MIMO system is obtained when low correlation exists between the multiple paths of the wireless channel. A rich multipath environment would ideally result in uncorrelated spatial characteristics at each antenna element. The PAS is just one spatial characteristic that may introduce channel correlation. Correlation between antenna elements in an array will also have a detrimental effect on the multiplexing capacity of the MIMO system.

It can be shown that the antenna-to-antenna spacing at either the transmitter and/or receiver has a strong relationship to the overall spatial correlation [3]. For example, if two omni-directional receive antennas with the same polarization were placed in very close physical proximity, there would most likely be a high degree of correlation at the outputs of these two antenna elements, even in the presence of a rich multipath environment. Unfortunately, many portable MIMO devices tend to be physically small, thus limiting the antenna separation to less than

a wavelength. An alternate solution to achieve the low spatial correlation between two closely spaced antennas is to cross polarize the antennas, or, in other words, position the antenna polarizations in orthogonal or near orthogonal orientations [3]. Additionally, low correlation may be achieved with pattern diversity in the antenna gains at the BS and/or UE. Figure 7a shows the simulated antenna gain pattern for each receive antenna element in a two-element dipole array. Figure 7a also shows the AoA for six signals arriving from clusters positioned in the surrounding environment. It is expected that the difference between the two antenna gain patterns may improve the capacity of the MIMO system when compared to a system having antennas with omni-directional patterns. For example, Figure 7b shows the simulated capacity for a 2x2 MIMO system using this two-element dipole array in the presence of a channel with a single cluster having a BS AoD of 50 degrees and AS of 2 degrees, and the UE having an AoA of 67.5 degrees and AS of 35 degrees. As shown in Figure 7b, the capacity is

higher when there is pattern diversity between the UE antenna elements as compared to the omni-directional case. The capacity found in this example was simulated using the correlation-based model implemented with a Laplacian PAS distribution and antenna patterns shown in Figure 7a. The dipole antenna patterns were modeled using the Agilent electro-magnetic solver EMPro. The capacity was calculated using the correlation coefficients determined by the Agilent N5106A PXB channel emulator. The PXB can calculate the channel coefficients from selected channel models and arbitrary antenna patterns. The PXB calculations can use either the correlation-based or geometry-based channel models. By providing a method to separate the PAS from the antenna patterns, MIMO system performance can be quickly evaluated using a variety of antenna arrays, even before the BS and UE antennas are built. The next section of the application note includes the mathematics for calculating the spatial correlation matrix by separating the antenna patterns from the spatial properties of the channel.

(a) Antenna pattern and cluster AoAs
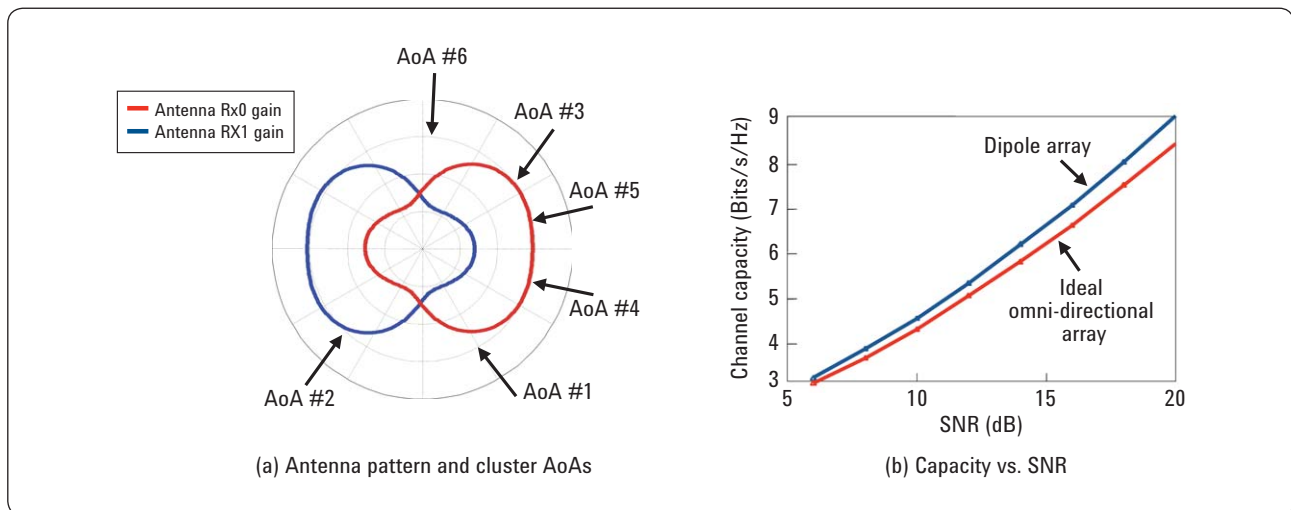
(b) Capacity vs. SNR

Figure 7. (a) Antenna pattern diversity operating in a multipath channel with six clusters. (b) MIMO capacity versus SNR using a dipole antenna array and an omni-directional antenna array having a single multipath cluster.

Modeling the capacity and spatial correlation of the multipath channel

The instantaneous capacity of an MxN receive antenna MIMO system can be expressed as the following equation:

$$C_{MIMO} = \log_2\left[\det\left(I_N + \frac{\gamma}{M} HH^H\right)\right] \quad (1)$$

Where I_N is the N-by-N identity matrix, γ is the average receive signal to noise ratio (SNR), $(.)^H$ is the complex conjugate transpose, and H is the normalized channel matrix which includes the spatial correlation effects of PAS and antenna gain patterns. Modeling a MIMO system using the geometry-based SCM method allows the individual channel

coefficients of H to be calculated directly by summation of the multiple sub-path characteristics between the pairs of transmit and receive antennas. In this case, the spatial effects of antenna gain can be handled by associating the AoAs and AoDs for each sub-path with the angular distribution of the gain pattern.

Obtaining the MIMO capacity using the correlation-based method first requires a calculation of the spatial correlation matrix, R, in order to calculate the channel matrix, H, and associated capacity. It will be shown that the spatial correlation matrix of the channel can be separated into a transmitter correlation matrix and a receiver correlation matrix.

While both the correlation-based and geometry-based methods are only approximations to the desired MIMO channel, it is important to understand

the assumptions and mathematics used in each technique. The following sections of this application note will review the mathematical techniques that allow separation of the spatial properties from the antenna characteristics. Separating the spatial and antenna properties allows the channel models to be implemented in a practical OTA test system. Comparisons will be made between practical implementations of several OTA measurement systems using either a correlation-based or a geometry-based model. As shown in the examples below, the two-stage OTA test method allows direct comparison between these two channel models while operating with the same hardware configuration.

Correlation-based model using independent spatial properties at the transmitter and receiver

As the capacity of a MIMO system substantially depends on the spatial correlation between individual transmit and receive branches, the spatial correlation matrix, R, is often a desired metric that provides an intuitive understanding of the system's operation. Under certain assumptions, the spatial correlation matrix at the transmitter side, R_{TX}, can be separated from the spatial correlation matrix at the receiver side, R_{RX}, allowing the complete spatial correlation matrix, R, to be calculated using the following equation:

$$R = \frac{1}{tr\{R_{RX}\}} R_{TX} \otimes R_{RX} \qquad (2)$$

Where tr{.} is the trace of the matrix and $\otimes$ is the Kronecker product. The Kronecker assumption has the advantage that the entries in the complete spatial correlation matrix can be separated into the transmitter side and receiver side [9].

The spatial correlations at the transmitter and receiver can be independently determined based on the PAS and antenna gain patterns at the respective antenna arrays. For example, using a simplified 2x2 MIMO model where the antenna element patterns, $G(\theta)$, are identical at the transmitter, the calculated transmit correlation coefficient between transmit antenna element 1 and transmit antenna element 2 is found using the following equation:

$$\rho_{TX,12} = \frac{\int_{-\pi}^{\pi} e^{-j2\pi \frac{d}{\lambda} \sin(\theta)} PAS_{TX}(\theta)G_{TX}(\theta)d\theta}{\int_{-\pi}^{\pi} PAS_{TX}(\theta)G_{TX}(\theta)d\theta} \qquad (3)$$

Where d is the physical distance between transmit antenna elements, $PAS_{TX}(\theta)$ is the power azimuth spectrum at the transmitter having a set of truncated Laplacian, uniform or Gaussian PDFs, $G_{TX}(\theta)$ is the antenna element pattern at the transmitter which is assumed identical for each, and λ is the carrier wavelength.

A similar equation can be used to determine the correlation coefficient at the receiver array. For this simplified example, it is assumed that the antenna element patterns at the receiver are identical, though the patterns between the transmitter and receiver could be different. The receive correlation coefficient between receive antenna element 1 and receive antenna element 2 is found using the following equation:

$$\rho_{RX,12} = \frac{\int_{-\pi}^{\pi} e^{-j2\pi \frac{d}{\lambda} \sin(\theta)} PAS_{RX}(\theta)G_{RX}(\theta)d\theta}{\int_{-\pi}^{\pi} PAS_{RX}(\theta)G_{RX}(\theta)d\theta} \qquad (4)$$

As shown in equations (3) and (4), the correlation coefficients at the transmitter and receiver are directly related to the multiplication of the PAS and the associated antenna gain. As a result, independent measurements of transmitter antenna gain and receiver antenna gain can be used to calculate the respective correlation coefficients. The correlation coefficients can then be used to determine the correlation matrix at the transmitter and receiver using the following equation:

$$R_{Tx} = \begin{bmatrix} 1 & \rho_{TX,12} \\ (\rho_{TX,12})^* & 1 \end{bmatrix} \qquad (5)$$

$$R_{Rx} = \begin{bmatrix} 1 & \rho_{RX,12} \\ (\rho_{RX,12})^* & 1 \end{bmatrix} \qquad (6)$$

Where $(.)^*$ is the complex conjugate. The complete channel correlation matrix, R, would be calculated using equation (2). The simplified expressions for correlation coefficients (3) and (4) assumed that the element patterns were the same at each location. If the element patterns were different, such as the case shown in Figure 7a, then the equations for correlation coefficients would need to be modified to include the effects of different antenna gain patterns. This technique is also robust enough to include the effects of antenna polarization. The spatial correlation matrices provide insight into the level of correlation to the signals leaving the transmit antenna array and the signals arriving at the receive array independently. As such, the spatial correlation matrices are often used to compare the performance of different OTA measurement techniques as shown later in this application note.

Continuing with the Kronecker assumption described above, the channel matrix can then be approximated using the following equation:

$$\hat{H} = \frac{1}{\sqrt{tr\{R_{RX}\}}} R_{RX}^{1/2} G \left(R_{TX}^{1/2}\right)^T \qquad (7)$$

Where $(.)^T$ is the matrix transpose and G is an N x M random matrix with zero-mean i.i.d. complex Gaussian entries. In general, the Kronecker assumption will result in a less accurate model of the short-term time variation of wideband channels [9] for arbitrary polarization angles. Agilent has developed a proprietary algorithm that improves the accuracy of the Kronecker assumption when calculating the spatial correlation matrix and channel matrix using the correlation-based method in a two-stage OTA measurement.

Geometry-based model using independent spatial and antenna gain parameters

When using the geometry-based channel model, such as the SCM, the channel matrix is calculated from the summation of numerous sub-paths associated with separate clusters placed in the channel. The geometry-based model, also called a double directional channel model, does not explicitly specify the locations of the individual clusters, but rather the angular directions of the sub-paths. Geometry-based modeling of the radio channel also allows separation of spatial parameters and antenna patterns. As shown in the correlation-based method, separation of the spatial and antenna characteristics will simplify calculation of the channel and correlation matrices. For the 3GPP SCM downlink, the received signal at the UE consists of six time-delayed paths from the transmitter. Each path consists of 20 sub-paths in an SCM simulation. As previously described, having 20 sub-paths results in a highly accurate representation of the PAS using the sum-of-sinusoids technique.

A simplified calculation for the coefficient of the mth sub-path within the nth cluster is shown in Figure 8. The coefficient calculation is based on the geometry shown in Figure 5 for a 2x2 MIMO system. The following calculation is associated with antenna pair Tx1 and Rx1. There would be a similar calculation for each antenna pair between all combinations of transmit and receive antennas.

The angle $\theta_{n, m, AoD}$ is defined as the AoD for the mth sub-path of the nth cluster, $\theta_{n, m, AoA}$ is the AoA for this sub-path, $G(\theta_{n, m, AoD})$ is the BS antenna gain at angle $\theta_{n, m, AoD}$, $G(\theta_{n, m, AoA})$ is the UE antenna gain at angle $\theta_{n, m, AoA}$, $\phi_{n, m}$ is the phase of the mth sub-path of the nth cluster and $k = 2\pi/\lambda$. The geometry-based model and associated calculation in Figure 8 shows that the antenna gains and the angular parameters are separable. This simplified calculation assumes no time variation as a result of propagation delay and UE motion, and no attenuation effects due to path loss and shadowing. A more complete expression including antenna polarization effects, loss and motion is included in reference [10].

The channel coefficient for the nth cluster between Tx1 and Rx1 is the summation of all the M sub-paths, where M is the total number of sub-paths in the sum-of-sinusoids approximation, typically set to 20. The complete channel coefficient for all N paths connecting Tx1 and Rx1 is the summation of coefficients for all individual clusters as shown below:

$$H(tx_1, rx_1) = \sum_{n=1}^{N} \sum_{m=1}^{M} h_{n, m}(tx_1, rx_1) \tag{8}$$

The number of clusters, N, is six in the 3GPP SCM. The complete channel matrix, H, for this simplified 2x2 MIMO system is then related to each combination of transmit to receive antenna pairs using the following equation:

$$H = \begin{vmatrix} H(tx_0, rx_0) & H(tx_0, rx_1) \\ H(tx_1, rx_0) & H(tx_1, rx_1) \end{vmatrix} \tag{9}$$

Having the complete channel matrix, the calculation of the spatial correlation matrix, R, is defined in reference [11] as:

$$R = E \left\{ vec(H) \, vec(H)^H \right\} \tag{10}$$

Here E{ } is the expected value. The calculation in equation (10) does not require the Kronecker product to determine the correlation matrix but still allows separation of the spatial properties and the antenna gains as shown in Figure 8. As mentioned, the above-simplified expression for channel matrix, H, does not include the effects of time due to motion and path delay. The actual time variant impulse response for the MIMO channel would have the form of $H(t;\tau)$, as shown in reference 3GPP Tdoc R4-091949 [10].

It will be shown when implementing the SCM in the multiple test probe OTA test system, that a reduction in hardware complexity and cost can be achieved using a smaller number of sub-paths at the expense of potential uncertainty in the measurements. When implementing the SCM model in the two-stage OTA system, all six paths, each with 20 sub-paths, can be easily implemented within the Agilent N5106A PXB at a greatly reduced system cost and complexity.

$$h_{n, m}(tx_1, rx_1) = \sqrt{G(\theta_{n, m, AoD})} e^{\, jkd_{tx} \sin(\theta_{n, m, AoD})} \sqrt{G(\theta_{n, m, AoA})} e^{\, jkd_{Rx} \sin(\theta_{n, m, AoA})} e^{\, j\phi_{n, m}}$$

Figure 8. Simplified calculation for the coefficient of the mth sub-path within the nth cluster.

OTA Testing of MIMO Devices

Testing the radiated performance of MIMO devices in a repeatable and controllable environment is very challenging. Conducted tests can be defined to measure the performance of MIMO receivers, however, tests may not emulate real life conditions if the effects of antenna and spatial radiation are not included as part of the test. The purpose of OTA testing is to include the radiated characteristics of the multipath channel and the MIMO antenna during the measurement process. OTA testing can be used to identify whether the MIMO antenna design has acceptable performance over a wide variety of multipath environments. One challenge to OTA testing is to select a multipath channel model that can be implemented in a practical measurement system without loss in accuracy. Of the two channel models discussed, correlation-based and geometry-based, several measurement configurations are available that approximate these models and effectively measure the radiated performance of the MIMO UE. It will be shown that different OTA measurement techniques will have approximately the same performance and the selection of the OTA test system should be based on the complexity, flexibility and cost to the end-user.

In the ideal case, testing MIMO devices would be as simple as testing SISO devices, but as discussed above, the MIMO performance is closely tied to the antenna performance and the channel's spatial characteristics, thus making MIMO OTA testing much more challenging and potentially complex. For example, the standardized OTA test method for a SISO device is conceptually simple, resulting in a set of basic measurements including antenna gain, TRS and TRP [5]. As shown in Figure 9, a typical configuration for measuring a SISO antenna gain includes an anechoic chamber and a vector network ana-

lyzer (VNA), such as the Agilent PNA Series or ENA Series analyzers. The antenna gain can easily be measured using the VNA when a direct connection to the UE antenna is available. For this configuration, a known reference antenna and an associated calibration procedure would be required to remove path loss from the transmission measurement. For a UE without internal access to the antenna, the UE could be placed in a test mode that supports capturing I/Q data or a channel estimate associated with the received signal. In this configuration, the VNA is replaced with a BS emulator when measuring receive gain and a signal analyzer for transmission gain. An Agilent E6621A BS emulator and N9020A MXA signal analyzer can be used in this environment. As the antenna gain is usually expressed as a function of spatial angle, the azimuth and elevation gain performance is measured while physically rotating the UE. Also, when polarization effects are required, the UE antenna or the reference antenna can be rotated by 90 degrees.

When measuring the TRS of the UE receiver, a BS emulator is connected to the reference antenna and a separate connection is made to the baseband control of the UE in order to measure bit-error-rate (BER), frame-error-rate (FER) and/or received power level. When measuring the TRP from the UE transmitter, a link antenna is connected to the BS emulator to independently control the operation of the UE while a signal analyzer is used to measure the transmitted power at the reference antenna. The TRS and TRP are typically averaged as the UE is physically rotated over various elevation and azimuth orientations to include the effects of antenna gain. In some cases, the UE is attached to a SAM phantom to measure the proximity effects to a human test model. In addition, these active measurements

can include time-varying effects of a multipath channel by including a channel fader such as the Agilent N5106A PXB baseband generator and channel emulator.

An important point concerning the accuracy of the anechoic chamber measurement is that while the anechoic material is typically constructed of pyramidal RF absorbers, the sum of all non-ideal internal reflections from these absorbers and surrounding support structures and test cables must be lower than the desired signal, otherwise these undesired reflections will decrease the accuracy of the radiated measurements. An anechoic chamber is designed to optimize a small area around the DUT with minimal internal reflections. This area is called the quiet zone of the anechoic chamber. This quiet zone is typically a function of the chamber size and operating frequency and is usually optimized so that the DUT would completely fit inside this area for the highest measurement accuracy. When measuring large DUTs or a DUT against a SAM phantom, the physical size of the chamber and associated quiet zone must be considered. Ideally, the quiet zone is positioned far enough away from any reference or probe antenna in order to approximate a far-field or plane-wave propagation of the radiated test signals. The far-field approximation would simulate the expected operating environment for the DUT.
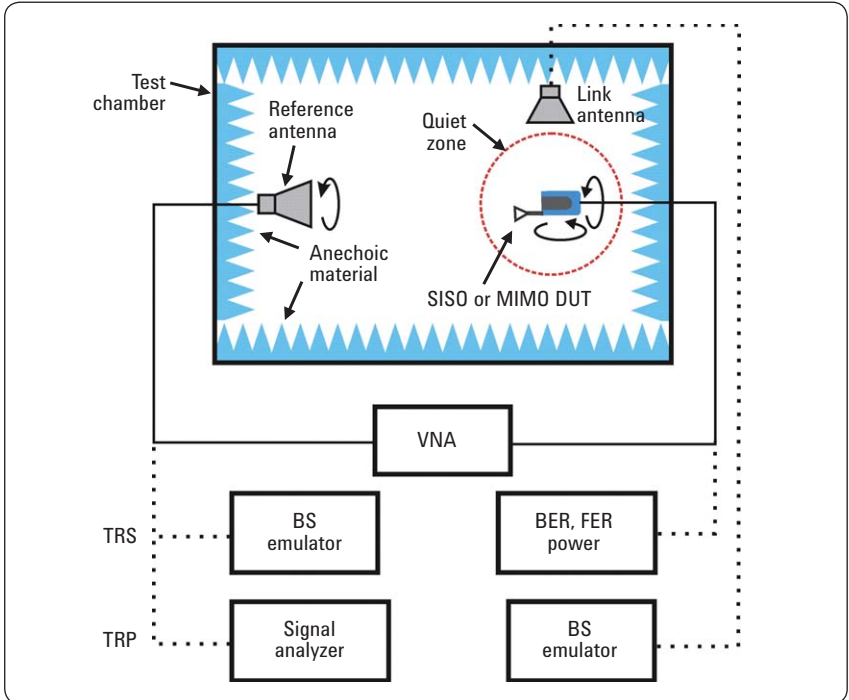
Figure 9. Basic OTA test configuration for measuring antenna gain, TRS and TRP of SISO and MIMO devices.

The test methodologies and metrics for a SISO OTA measurement cannot be directly extended to a MIMO OTA test system if the interactions between channel and antenna characteristics are to be included. For the MIMO antenna, not only will the received power imbalance at each antenna influence the performance, but also the spatial correlations. As previously discussed, the correlation depends on antenna parameters, such as gain, element spacing and element polarization as well as PAS parameters such as AoA, AoD and AS. The major challenge for MIMO OTA performance testing is to find a measurement method that includes the radiated performance of the MIMO antenna while operating in a realistic multipath environment. As previously shown, both the correlation-based and geometry-based models allow the antenna gain and the channel's spatial properties to be independently determined and

used to estimate the MIMO capacity. This technique will provide a useful method for measuring the OTA performance of a MIMO device.

Various systems and methods have been proposed to generate realistic propagation environments for MIMO OTA testing. Three of the major test methodologies will be addressed in the following sections of this application note. One of the methods requires a reverberation chamber to generate a rich propagation environment [6], but this technique is limited to uniform PAS. A second method requires multiple probe antennas surrounding the UE inside the anechoic chamber and, together with channel emulation, can achieve a variety of multipath conditions [6]. The issue with the multiple test probe OTA method is that the number of probe antennas and RF channel emulators rapidly becomes very large in order to achieve good accuracy. Add in the

capability for polarization diversity, and the resulting OTA test system may be very complex and costly. The third method is an extension over traditional antenna gain measurements where the radiated performance of the MIMO antenna is first measured using a standard anechoic chamber. The second step in this method combines the measured OTA antenna performance with the desired channel model using a channel emulator such as the Agilent N5106A PXB. The desired FOMs for the MIMO UE are then determined using a conducted measurement having a direct connection between the UE and the emulator. This two-stage OTA method [6] is described in the next section of this application note.

MIMO OTA testing using the two-stage method

The two-stage OTA method is designed to provide an accurate and cost effective MIMO OTA measurement system by combining the benefits of traditional anechoic chamber radiated measurements with the flexibility of a fading channel emulator, such as the Agilent N5106A PXB. The two-stage method is based on the knowledge that the antenna characteristics can be independently measured and then mathematically combined with the desired channel characteristics in the Agilent N5106A PXB channel emulator. As shown in equations (3) and (4) for the correlation-based model, the respective antenna gains at the transmitter and receiver are independent factors in the determination of the spatial correlation coefficients and the associated channel coefficients. A similar approach is found when using the geometry-based model. As shown in equation (8), the antenna gain can also be introduced as an independent parameter in the determination of channel coefficients. One benefit to the two-stage method is that either channel model, correlation-based or geometry-based, can be produced by the PXB channel emulator. By measuring both models using the same hardware and measured antenna gain patterns, it is possible to compare the MIMO performance using both channel models. Details for implementing the two-stage OTA method follow.

The first stage in the two-stage OTA method requires measurements of the antenna array gain pattern with the UE placed inside a standard anechoic chamber as shown in Figure 10. The array gain can be passively measured using a VNA, such as the Agilent PNA Series or ENA Series analyzers, when direct access to the UE antenna ports is available. When antenna ports are not available, the UE array gain can be actively measured using a BS emulator, and a UE capable of providing I/Q

data or channel estimates. During UE transmit array gain measurements, the BS emulator can be connected to a link antenna, as shown in Figure 9, As in the SISO case, the chamber should be equipped with a positioner, making it possible to perform full 3-D far-field pattern measurements for both the transmit and receive antenna arrays. The reference antenna should also be capable of measuring two orthogonal polarizations either through physical movement of a linearly-polarized antenna or through a pair of cross-polarized antennas. For the MIMO pattern testing, the equipment and chamber requirements are the same as that of a SISO antenna measurement. Once the antenna patterns are measured, they can be used by the channel emulator to reproduce the UE antenna influence during the second stage of MIMO testing.

The second stage in the two-stage OTA method requires a conducted test of the UE using a BS emulator and a channel emulator, such as the Agilent N5106A

PXB. The channel emulator combines the actual measured or simulated 2D or 3D antenna gains with the selected MIMO channel model. The model can be based on either the correlation or geometry approximations of a rich multipath environment. The lower portion of Figure 10 shows the measurement configuration for this second stage of UE testing. In this figure, a 2x2 MIMO system is measured using a four-channel fading emulator. In general, as the number of fading channels in the emulator equals the number of transmitters times the number of receivers at the UE, the two-stage OTA method is one of the most cost effective techniques. The output from the two-stage method may include BER, FER, channel coefficients and correlation coefficients. From these metrics the channel capacity can also be calculated. It should be noted that the two-stage method is capable of characterizing a MIMO device for all the FOM requirements previously shown in Table 1 [12].
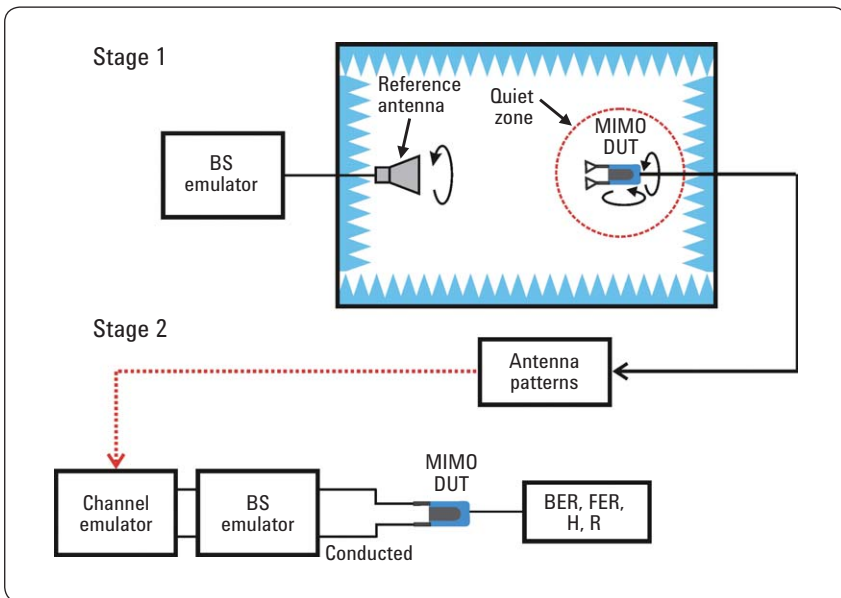

Figure 10. Test configuration using the two-stage OTA method for a 2x2 MIMO device. Stage 1 requires measurements of array gain and Stage 2 combines the gain measurements with the channel model in a conducted performance test.

There are several considerations required when implementing the two-stage OTA method. The first consideration is related to the correlation-based model and the associated Kronecker product used to separate the transmitter correlation matrix from the receiver correlation matrix as shown in equation (2). Agilent has found that for real antenna patterns, the Kronecker assumption is not typically valid and thus becomes an issue when attempting to combine the antenna patterns with channel model. Agilent has developed a unique correlation matrix calculation for arbitrary antenna patterns under multipath channel conditions that improves the accuracy of the Kronecker approach. Another consideration in the two-stage MIMO OTA method is that the far field UE antenna patterns can be accurately measured in order to fully capture the mutual coupling between the multiple antenna elements. This can be accomplished with careful calibration of the anechoic chamber test system. One last consideration in the two-stage OTA method concerns the physical connection to the UE receiver ports during the conducted test stage. The UE must have the capability to bypass the antennas and provide a cabled connection to the channel emulator as shown in Figure 10. While this technique is especially attractive during the development phase of the UE, by allowing the ability to quickly measure the MIMO performance with various antenna configurations, it assumes that there is minimal interaction between internal spurious emissions from UE radio hardware and the MIMO antenna array.

As a comparison between a correlation-based channel model and the equivalent geometry-based model using only the two-stage OTA test system, Table 3 shows the resulting correlation coefficients for the two channel models. The MIMO system used vertically polarized omni-directional antennas at the BS array with a single cluster modeled as a Laplacian PDF and AS of 2 degrees. The UE array consisted of vertically polarized dipole antennas with antenna patterns shown in Figure 7a and a single Laplacian PDF with AS of 35 degrees. The antenna separation at the BS and UE are two wavelengths and 0.225 wavelengths respectively.

The geometry-based SCM model implemented 20 sub-paths for the single cluster and 50 drops were used to provide a statistical average of the matrix coefficients. The mean AoD and AoA were changed for each drop and randomly distributed over 360 degrees. As shown in Table 3a and 3b, the correlation coefficients for the respective transmit and receive antenna pairs are very close in value. Table 3c shows the differences between these matrices. Most of the values in Table 3c are negative, which means that the correlation coefficients from the SCM model are slightly lower than the correlation-based channel coefficients.

Table 3a. Channel correlation matrix from SCM

	Tx0-Rx0	Tx0-Rx1	Tx1-Rx0	Tx1-Rx1
Tx0-Rx0	1.0000	0.6670	0.9519	0.6687
Tx0-Rx1	0.6670	1.0000	0.6496	0.9550
Tx1-Rx0	0.9519	0.6496	1.0000	0.6672
Tx1-Rx1	0.6687	0.9550	0.6672	1.0000

Table 3b. Channel correlation matrix from correlation-based model

	Tx0-Rx0	Tx0-Rx1	Tx1-Rx0	Tx1-Rx1
Tx0-Rx0	1.0000	0.7050	0.9547	0.6721
Tx0-Rx1	0.7050	1.0000	0.6721	0.9547
Tx1-Rx0	0.9547	0.6721	1.0000	0.7050
Tx1-Rx1	0.6721	0.9547	0.7050	1.0000

Table 3c. Difference between SCM and correlation-based model (Table 3a –Table 3b)

	Tx0-Rx0	Tx0-Rx1	Tx1-Rx0	Tx1-Rx1
Tx0-Rx0	0	-0.0380	-0.0027	-0.0034
Tx0-Rx1	-0.0380	0	-0.0225	0.0003
Tx1-Rx0	-0.0027	-0.0225	0	-0.0378
Tx1-Rx1	-0.0034	0.0003	-0.0378	0

To create a measurement example of the MIMO capacity as a function of the UE orientation using the two-stage OTA test method, a commercial MIMO USB dongle was connected to a pair of dipole antennas. The measured antenna pattern for each element is shown in Figure 11a. The antenna patterns were also measured against a SAM phantom with the results shown in Figure 11b. It is noted that there are large changes to the measured dipole patterns in the presence of the SAM head model and it is expected that this will greatly affect the MIMO performance. The two-stage OTA method implemented the rural macro SCM running inside the Agilent N5106A PXB channel emulator [13]. The antenna patterns were incorporated into the channel model and the MIMO capacity was estimated with the UE rotated over 180 degrees in 10 degree steps. The measured MIMO capacity is shown in Figure 11c, illustrating that the SAM phantom not only has a large influence on the antenna gain patterns, but also on the measured capacity as a function of UE orientation. Additional measurement examples for spatial correlation and channel capacity using the two-stage OTA method will be compared to the multiple test probe OTA method later in this application note.
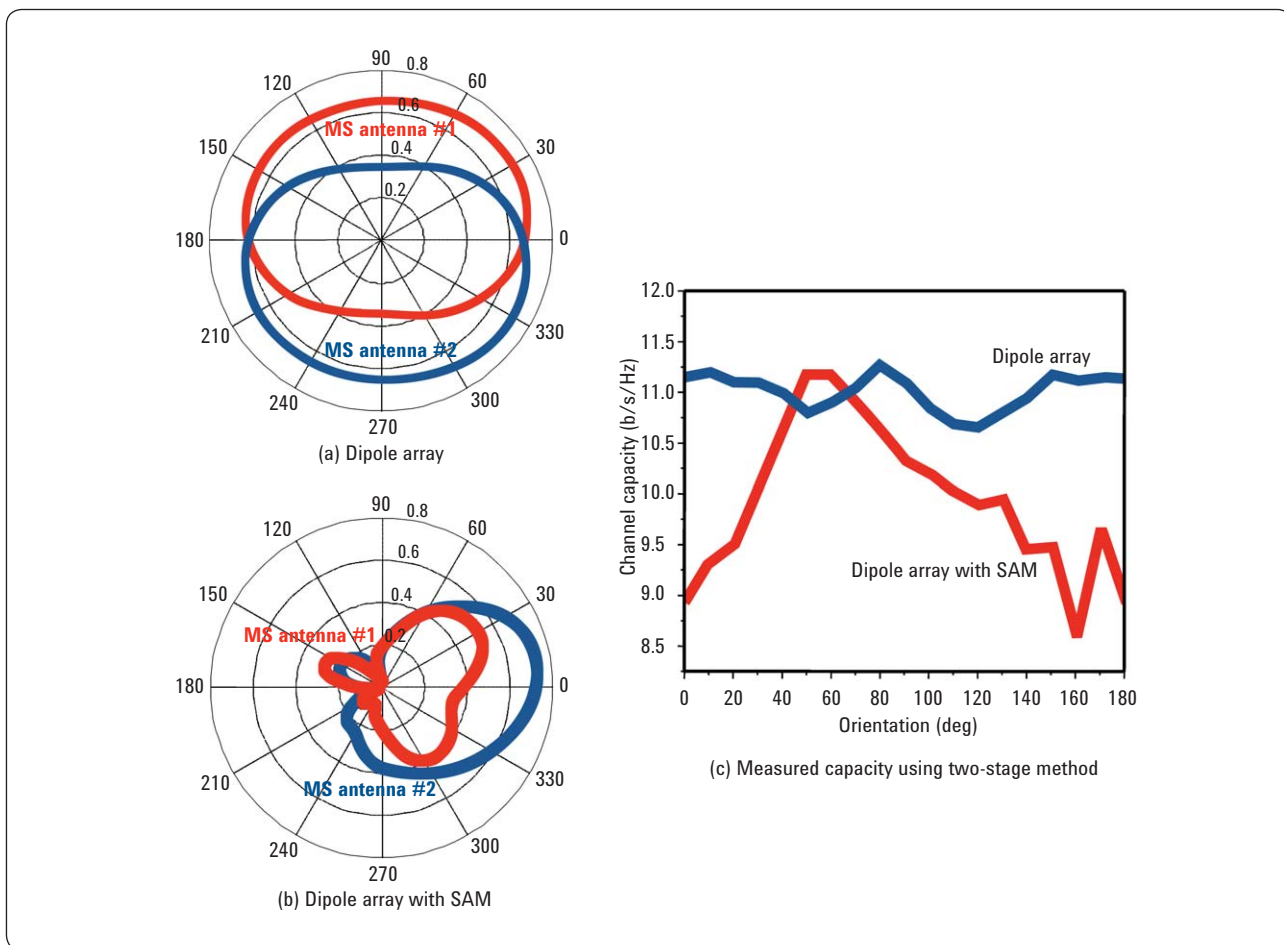
Figure 11. (a) Measured antenna patterns for a 2-element dipole array using the two-stage OTA method, (b) measured antenna pattern for the same array in the presence of a SAM phantom and (c) measured 2x2 MIMO capacity using these two arrays at the UE.

MIMO OTA testing using multiple test probes

A second OTA test method using an anechoic chamber includes a large set of probe antennas placed within the chamber and positioned around the MIMO DUT. The multiple test probe OTA method attempts to emulate the receive-side AoA and AS characteristics that would be radiated from several multipath clusters. The spatial characteristics from the BS, such as AoD and AS, are emulated using a channel emulator such as the Agilent N5106A PXB and associated MXG signal generators connected to

the multiple test probes. This OTA method approximates a MIMO channel using a geometry-based channel model such as the 3GPP SCM. Figure 12 shows the configuration of the multiple test probe OTA test system using an anechoic chamber with eight probe antennas placed uniformly around the MIMO UE. Each probe antenna emulates a sub-path in the geometry-based cluster model. Several test probes are often grouped to approximate the AS of a single cluster. The probes are excited at different angular positions around the UE to emulate a specific AoA. While radiation from the probes approxi-

mate the OTA signals arriving at the UE, individual channel emulators are cabled to each probe to emulate the effects of BS spatial correlation, path delay, path fading and Doppler. If dual polarized antenna measurements are required, the number of probe antennas and channel emulators would double. Figure 12 shows a BS emulator and a channel emulator, such as the Agilent N5106A PXB, configured to create the faded test signals for each sub-path, as well as a set of Agilent MXG signal generators to upconvert the faded baseband signals to the required RF carrier frequency.
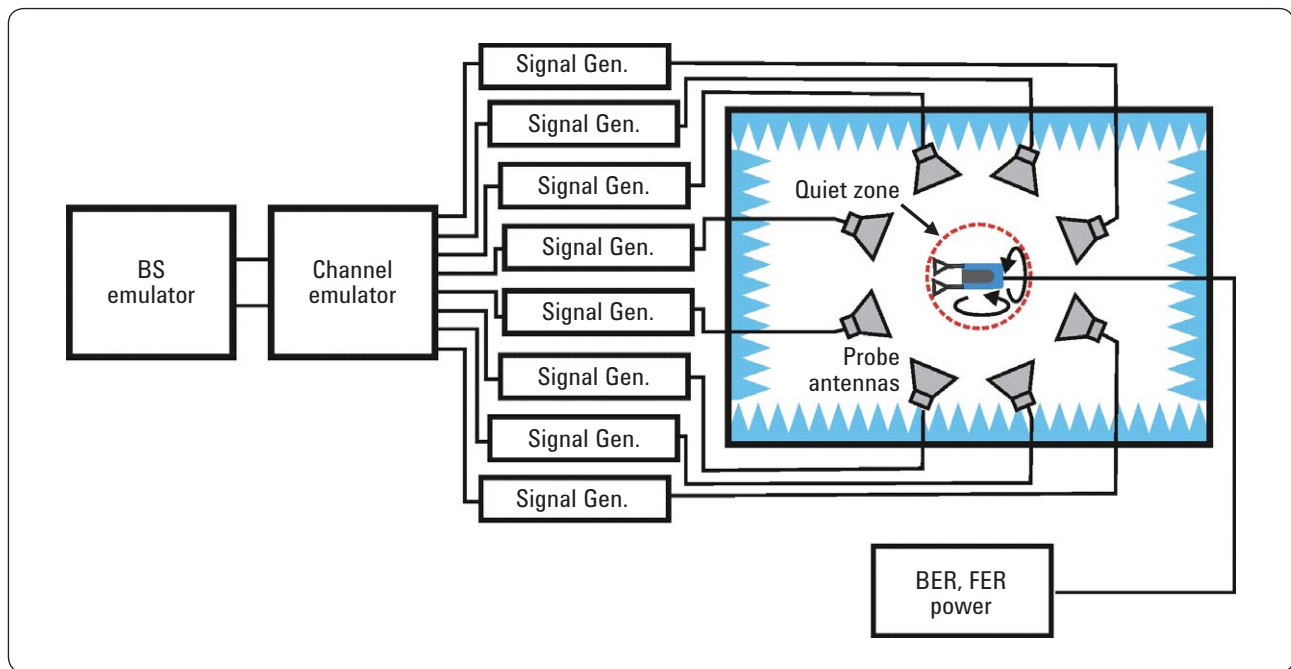
Figure 12. Test configuration for the multiple test probe OTA method using an anechoic chamber and channel emulator. Probe antennas are grouped to emulate the desired AoA and associated AS.

There are several challenges facing OTA test methodologies that attempt to fully emulate multipath fading using multiple probe antennas within an anechoic chamber. As previously mentioned, geometry-based approximations to a MIMO channel can be implemented using either a sum-of-sinusoids technique or a quantized PAS with unequal amplitude sub-paths. Due to practical concerns over equipment complexity, lengthy calibration and test times, as well as potential high cost, a reduced number of test probes is often preferred, resulting in the use of the quantized PAS approximation for the channel model. When approximating the PAS with a limited number of test probes, the probe spacing and power levels need to be optimized in order to achieve a realistic test environment. System simulations have shown that a reasonably accurate test method can be achieved with a reduced number of test probes. For example, a simulation using three test probes grouped together to represent one cluster in the channel model showed that the simulated channel characteristics are very close to the theoretical model that used 20 sub-paths. In this case, the simulated and theoretical channel characteristics were compared for spatial correlation coefficient, Rayleigh statistics and fade depth [14]. It will be shown that measured results using three test probes will not be as accurate as the simulations, possibly due to sensitivity to errors in chamber calibration and probe location. Measured throughput data using this configuration will be provided later in this application note along with comparisons to the two-stage OTA method.

Another challenge to implementing the multiple test probe OTA method includes optimization of the anechoic chamber's quiet zone. It is also known that the size of the quiet zone can be increased with the introduction of additional test probes. The size of the quiet zone should be approximately one wavelength when testing UE handsets but would need to increase to approximately four wavelengths when testing laptops or a handset attached to a SAM phantom [15]. In this case, the chamber may be physically larger using the multiple test probe OTA method than a chamber required for traditional SISO and the two-step OTA method.

Agilent has measured the throughput of a commercially available MIMO device using the multiple test probe OTA method having a single cluster channel model with a Laplacian PAS and AS of 35 degrees at the UE. Figure 13a shows the test configuration using four probe antennas, representing four sub-paths, at a 40 degree angular spacing, and centered on the desired AoA. Using a simulation for this specific test configuration, the relative power levels across the four probes were optimized to match the statistics of a theoretical model based on the 20-path sum-of-sinusoids approach. As the total power level over all antennas is normalized to one, the simulated power levels resulted in a relative power of 0.13 for antennas #1 and #4 and 0.37 for antennas #2 and #3. Figure 13b shows the angular and power distribution for each sub-path in the quantized PAS implementation. It should be noted that the signals applied to each probe have independent Rayleigh fading statistics created using a four-channel Agilent N5106A PXB fading emulator and four MXG upconverters. The test system was calibrated using a known reference antenna to account for variation in the path loss as a function of angle for each test probe. The MIMO DUT was an 802.11n network card with two antennas. The TCP/IP throughput was measured as a function of angle at three power levels over the range of -34 dBm to -14 dBm. Figure 14 shows the measured throughput for this single cluster channel as the DUT was rotated over 360 degrees in the horizontal plane at 30 degree increments. As shown in the figure, the measured throughput is sensitive to AoA and power level. As expected, the measured results show that throughput can be quite high when the received power level, and associated SNR, is also high at each MIMO antenna. During the testing phase, it was discovered that the statistical average for throughput converged only when a very large number of measurement points were taken for each position of the DUT. It should be noted that, for the same fading model (sum of sinusoids), the measurement times are comparable between the multiple test probe OTA method and the two-stage OTA method. It should also be noted that the setup and calibration time of the anechoic chamber using the multiple test probe OTA method is typically 1-2 days while the chamber calibration and antenna measurements are complete in approximately 1 hour using the two-stage OTA method.

(a) Probe antenna configuration   (b) Laplacian approximation
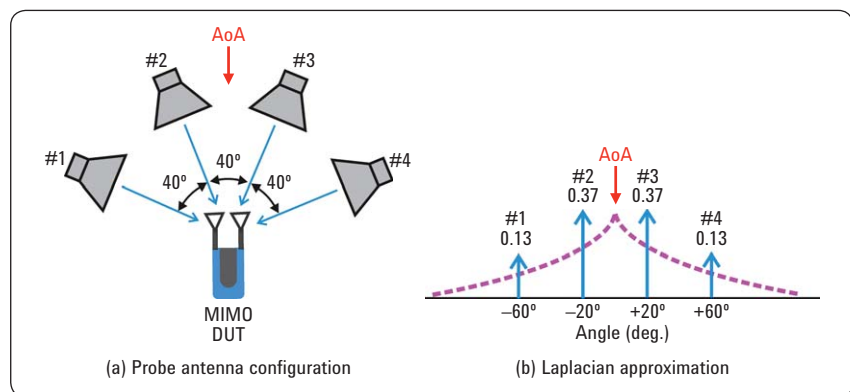
Figure 13. Probe antenna angular configuration and relative antenna power weights to approximate a single Laplacian PAS with AS of 35 degrees.

A second set of throughput measurements using the configuration shown in Figure 15a was performed with a channel having two multipath clusters. In this case, the four test probes will be shared between the two clusters. The relative cluster delay is set to 200 ns using the PXB channel emulator. As shown in Figure 15a, the AoA for each cluster is centered on probe antennas #2 and #3, respectively. For this configuration, the AS for each cluster is emulated using three probe antennas, and the power weights are chosen to maintain a 35 degree AS. The narrow spread of the AoA requires that two of the probes, #2 and #3, combine signals from both clusters. The test probes' relative angular positions and power weights are shown in Figure 15b. In this configuration, probe antennas #1-#3 are associated with AoA1 and have relative power weighting of 0.26, 0.48 and 0.26 respectively. Probes #2t-#4 have the same relative power distribution.

The measured throughput for the same MIMO device is shown in Figure 16. When the power level is set to -14dBm, the two-cluster channel model achieves a much higher throughput than single cluster model, confirming that a richer multipath channel will improve the MIMO performance. When the power level is reduced to -24 dBm and -34 dBm, the results for the two-cluster channel are very similar to the single cluster channel model, but with slightly lower throughput for the two-cluster channel. The difference between the measurements is due to the uncertainty of the TCP/IP throughput estimates. At these lower power levels, the receiver SNR is too low for MIMO multiplexing to be effective, and switching to beamforming and/or other antenna diversity techniques may improve the system performance.
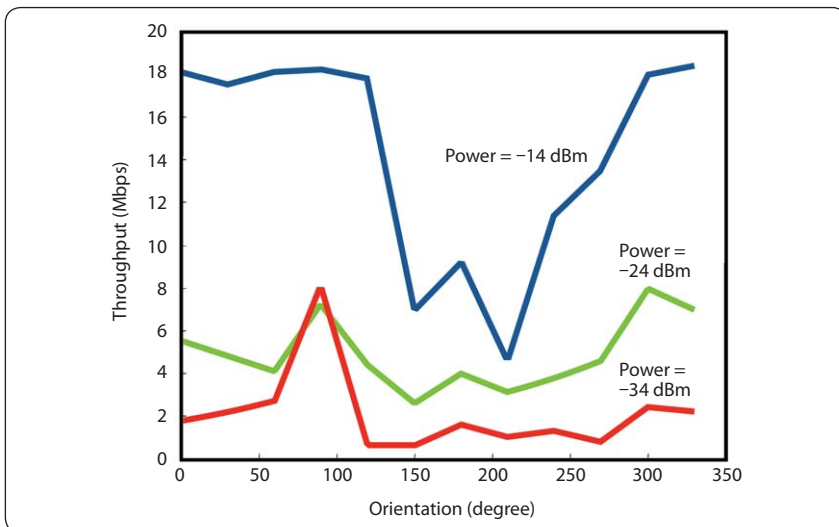
Figure 14. Measured throughput for commercial MIMO device using for single cluster channel.
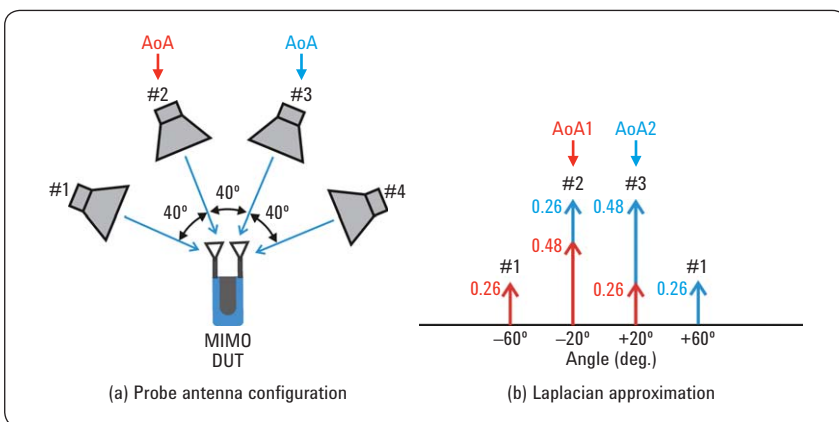
Figure 15. Probe antenna angular configuration and relative antenna power weights to approximate a two-cluster Laplacian PAS with AS of 35 degrees.
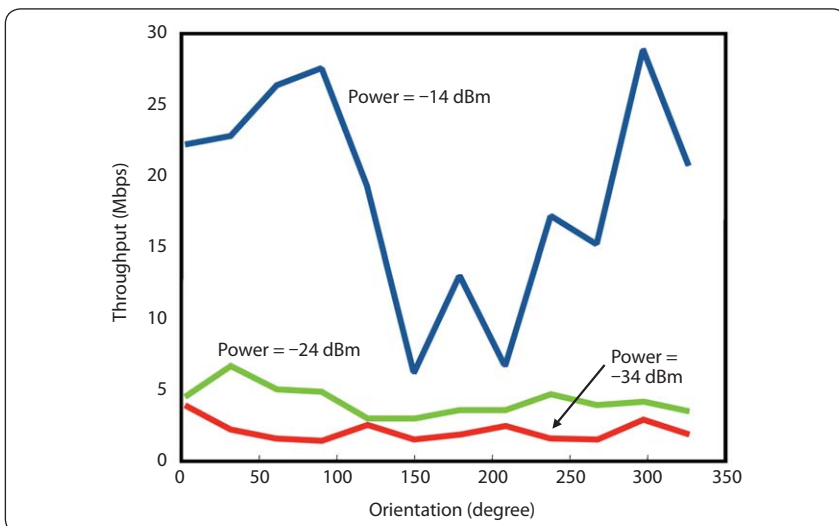
Figure 16. Measured throughput for commercial MIMO device using a two-cluster channel with relative 200 nsec excess delay.

MIMO OTA testing using a reverberation chamber

A third OTA measurement technique that has been proposed to evaluate MIMO performance operating in realistic fading channels makes use of a reverberation chamber. A reverberation chamber is a large metal cavity without absorbers that is sized to support numerous cavity modes. The modes are stirred with metallic plates that rotate or move during the testing phase. Movement of the plates will create Rayleigh distributed signal paths between reference antennas and the MIMO DUT. Figure 17 shows the configuration for measuring the OTA performance of a 2x2 MIMO system using a reverberation chamber with two wall antennas. The inside of the chamber is completely metallic and shielded from any extraneous signals. The number of wall antennas is the same as the proposed number of BS antennas. In Figure 17, the two BS antennas are connected to a BS emulator. Figure 17 also shows a single metallic mode-stirrer, but often several stirrers are required to move or rotate during OTA test. In addition, the MIMO UE may be placed on a rotating platform to improve the chamber's fading performance. The reverberation chamber and associated mode-stirrers create a three-dimensional uniform Rayleigh fading environment around the UE. The interaction between the BS antennas and the metallic cavity will influence antenna correlations. OTA measurements using a reverberation chamber resulted in a higher MIMO capacity when compared to the two-stage OTA method [16]. The difference may result from the fact that the reverberation chamber presents a uniformly distributed PAS in three-dimensions that is optimized for an indoor environment, especially when compared to a channel that is modeled for an outdoor environment. On the other hand, the reverberation chamber is useful when evaluating MIMO devices targeted for indoor environments where the spatial distributions tend to result in three-dimensional PAS distributions.

To improve the capability of the reverberation chamber OTA method, a channel emulator can be used to introduce an increased power delay profile (PDP), Doppler spectrum and spatial correlation at the BS antennas [6]. In this case, the basic measurement configuration is identical to the configuration shown in Figure 17, but the Agilent N5106A PXB introduces channel fading of the BS transmitted signals. It should be noted that the combined channel characteristics are a convolution of the reverberation chamber's multipath channel and the channel created by the channel emulator. In general, reverberation chambers tend to be physically smaller and lower cost than anechoic chambers. Since the channel is isotropic, there is no need to rotate the DUT during the test, thus the total measurement time using a reverberation chamber will be the shortest of the three OTA methods. When attempting to compare the measured spatial correlation between different OTA methods, the limited flexibility in configuring the AoA and AS when using the reverberation chamber method makes it difficult to compare these results to the measurements recorded using other OTA systems. However, the reverberation chamber has demonstrated the ability to rank-order devices equipped with receive diversity according to their relative throughput performance.
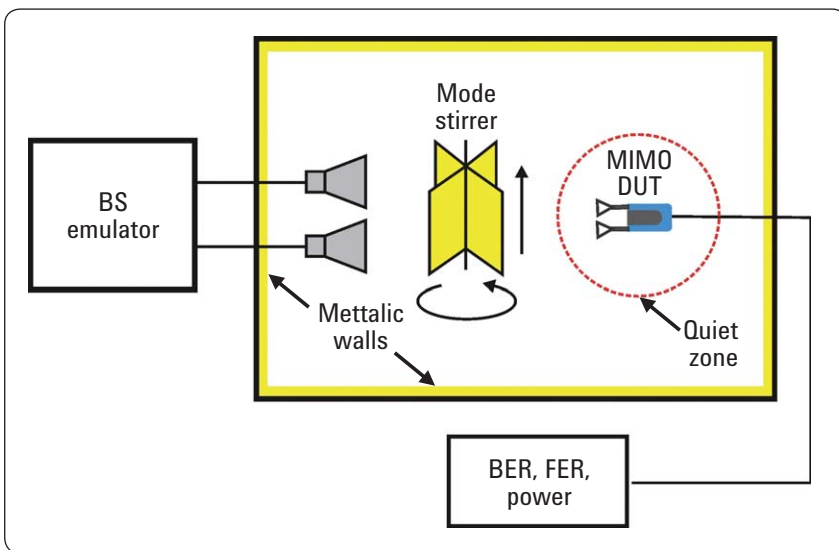

Figure 17. Test configuration for a 2x2 MIMO system using a reverberation chamber.

Experimental Validation of the Two-Stage and Multiple Test Probe OTA Methods

To compare the measured performance using the two-stage OTA method and the multiple test probe OTA method, a 2x2 MIMO system is implemented using a two-cluster channel model with Laplacian PAS and AoAs at -27.2 and +27.2 degrees and AS of 35 degrees [17]. The two-stage method is configured using the system described in Figure 10 and the multiple test probe method is configured using the system shown in Figure 12, but is implemented with only four test probes as shown in Figure 15. For all measurements, the OTA test systems were configured with vertically polarized antennas. In this case, the multiple test probe method required twice the number of PXB channels and signal generators than the two-stage method. If both vertical and horizontal antenna polarizations were required, then the multiple test probe method would require four times the number of PXB fading channels and signal generators. When measuring both polarizations using the two-stage system, the only addition is to include the measurement of vertical and horizontal antenna patterns during the first stage of test. It is this reduced system complexity and cost that makes the two-stage OTA method an attractive solution when characterizing MIMO device performance.

For these measurement comparisons, the two-stage OTA method begins with basic antenna pattern measurements of the two UE antennas tested over an angular range of ±180° in azimuth. The next step in the two-stage method is to combine the antenna patterns with the desired two-cluster channel model inside the Agilent N5106A PXB channel emulator. The two-stage method implemented two different channel models: the first model where the PXB creates the desired two-cluster multipath environment using a correlation-based Laplacian PAS and a second model where the PXB implements a geometry-based SCM using a 20 sub-path sum-of-sinusoids approximation.

The multiple test probe OTA method implemented the two-cluster channel model using a quantized PAS mapped to four antennas positioned around the UE as shown in Figure 15. For this measurement, the angular separation between test probes was set to 54.4 degrees noting that Figure 15 shows the separations at 40 degrees. The change in angular position required a complete recalibration of the path loss and readjustment of the probe power levels in order to achieve reasonable approximation between the quantized PAS and the desired SCM using 20 sub-paths. As shown in Figure 15, each cluster is approximated using three Rayleigh faded sub-paths [17]. Rayleigh fading is created at each test probe using a separate channel from the Agilent N5106A PXB. Also included is a simulation of a quantized Laplacian PAS model, as implemented in the multiple test probe system. This theoretical simulation is included as a comparison between all three measured results.

The real and imaginary components for the measured and theoretical spatial correlation between the two UE antennas as a function of UE orientation are shown in Figure 18. Comparing the test results between the two models implemented in the two-stage OTA method, the correlation coefficient terms using the geometry-based SCM are nearly identical to those using the correlation-based model implying that the sum-of-sinusoids technique using 20 sub-paths has similar measurement accuracy to the correlation-based model. The theoretical simulation of the quantized Laplacian PAS having three Rayleigh faded sub-paths also demonstrates reasonable tracking to the measured results using the two-stage OTA system. The measurements using the multiple test probe OTA method shows the largest discrepancy when compared to the other results. It is probable that the measurement accuracy using the quantized PAS approximation is sensitive to uncertainty in the chamber calibration and probe location. Increasing the number of test probes will improve the measurement accuracy at the expense of greater system complexity and higher implementation cost.
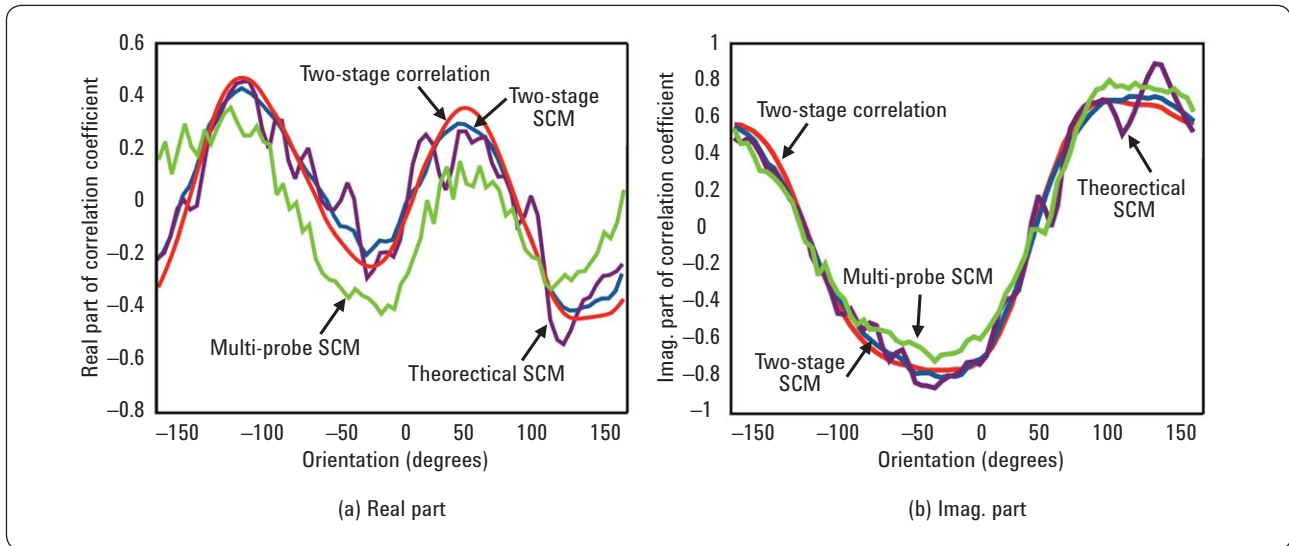
Figure 18. Real (a) and imaginary (b) components of the correlation coefficient between two UE antennas as a function of orientation angle.

The last set of measurements compare the average throughput of the commercial two-antenna HSDPA MIMO network card using the two-stage OTA method and the multiple test probe method. The throughput measurements were made with the card configured for 1x2 diversity and Hset 3. The maximum possible throughput in this configuration is 2332kbps. Figure 19 shows that the two measurements are effectively the same. While it is unlikely that throughput measurements will ever be identical using the same MIMO device tested under different OTA methods, the important requirement is that the selected OTA system is capable of determining a "good" MIMO device from a "bad" one. In addition, the selected OTA test system will require a trade-off between measurement speed, cost, system complexity and realistic operating conditions.

Throughput comparison Dell E6400 Single cluster, AS=35, V=3km/h
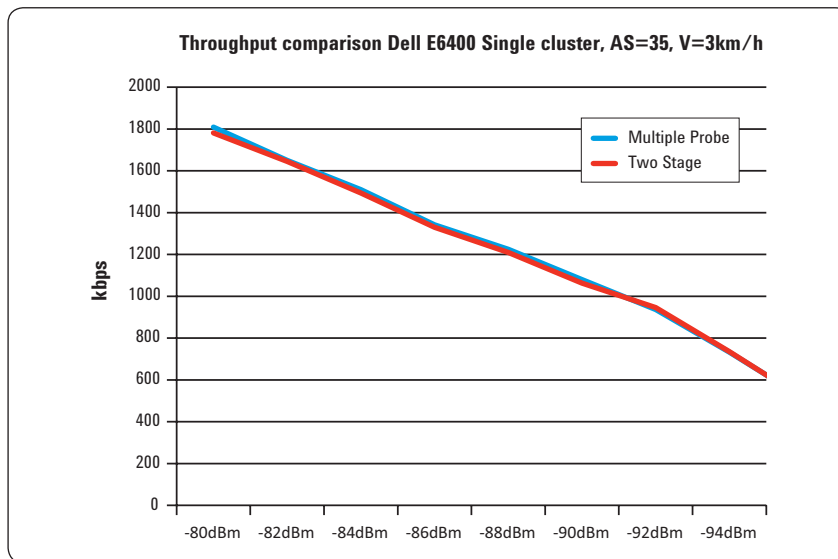
Figure 19. Comparison of the measured MIMO throughput using the two-stage OTA method and the multiple test probe OTA method.

Conclusion

This application note outlined the channel models and test methods for measuring the performance of MIMO devices in realistic environments using over-the-air test conditions. Three predominant OTA methods were described and test results were presented. While the reverberation chamber method is one of the fastest and lowest-cost OTA measurement techniques, it is limited to uniformly distributed multipath channels. The multiple test probe OTA method has the flexibility of emulating a variety of multipath conditions and does not require access to the UE antenna ports, however, this method can become highly complex and costly to implement especially when dual polarized antenna measurements are required. The multiple test probe OTA method also has the longest calibration and measurement times as well as the largest chamber requirements of the three OTA systems examined. The complexity and cost of the multiple test probe system can be reduced when using a smaller number of probe antennas, but system accuracy becomes sensitive to calibration and measurement errors. The two-stage OTA method comes closest to emulating the full mathematical models for a MIMO channel with a choice of either the correlation-based or geometry-based channel model. The two-stage OTA method has the advantage of reduced complexity and cost as well as faster system calibration and test time when compared to the multiple test probe method. The disadvantages to the two-stage OTA method are the required access to the antenna ports and the lack of potential receiver-to-receiver cross-coupling and antenna interactions. Even with these short-comings, excellent correlation exists between the two-stage OTA method and the multiple probe OTA method using commercially available MIMO devices.

References

[1] Agilent Application Note, "MIMO Wireless LAN PHY Layer [RF] Operation & Measurement," April 2008, 5989-3443EN

[2] Agilent Application Note, "MIMO Receiver Test Accurately Testing MIMO Receivers Under Real-World Conditions," January 2010, 5990-4045EN

[3] Agilent Application Note, "MIMO Channel Modeling and Emulation Test Challenges," January 2010, 5989-8973EN

[4] 3GPP TR 25.996 v6.1.0 (2003-09) 3rd Generation Partnership Project; Technical Specification Group Radio Access Network; Spatial channel model for Multiple Input Multiple Output (MIMO) simulations (Release 6)

[5] 3GPP TS 34.114 V8.3.0 (2009-12) Technical Specification 3rd Generation Partnership Project; Technical Specification Group Radio Access Network; User Equipment (UE)/Mobile Station (MS) Over-The-Air (OTA) antenna performance; Conformance testing (Release 8)

[6] 3GPP TR 37.976 V1.1.0 (2010-05) "Measurement of radiated performance for MIMO and multi-antenna reception for HSPA and LTE terminals" (Release 10)

[7] Kermoal, J.P.; Schumacher, L.; Pedersen, K.I.; Mogensen, P.E.; Frederiksen, F., "A stochastic MIMO radio channel model with experimental validation," IEEE Journal on Selected Areas in Communications, Volume 20, Issue 6, 2002, Page(s): 1211 – 1226

[8] 3GPP TR 25.996 V6.1.0 (2003-09) Spatial channel model for Multiple Input Multiple Output (MIMO) simulations (Release 6)

[9] Xiao, H., Alister G., "Full channel correlation matric of a time-variant wideband spatial channel model," The 17th Annual IEEE International Symposium on Personal, Indoor and Mobile Radio Communications (PIMRC'06), 2006

[10] 3GPP TSG-RAN WG4, Tdoc R4-091949, Agilent Technologies, "Applying measured MIMO antenna patterns to MIMO channel models for OTA analysis," San Francisco, CA, May 2009

[11] Ozcelik, H.; et al, "Deficiencies of 'Kronecker' MIMO radio channel model," Electronics Letters, Volume: 39, Issue: 16, 2003

[12] COST 2100 TD(09) 924, Agilent Technologies, "Two-stage MIMO OTA method," Vienna, Austria, Sept. 28-30, 2009

[13] COST 2100 TD(10) 10049, Agilent Technologies: "Test MIMO Antenna Effects on a MIMO Handset Using Two-stage OTA Method," Athens, Greece, Feb. 3-5, 2010

[14] 3GPP TSG-RAN4 R4-091362, Spirent Communications:"Practical MIMO OTA Testing," Seoul, Korea, March 2009

[15] 3GPP R4-094678, Elektrobit:, Optimum number of antennas in MIMO OTA system, Jeju, Korea, November 9 – 13, 2009

[16] Garcia-Garcia, L., et.al., "MIMO capacity of antenna arrays evaluated using radio channel measurements, reverberation chamber and radiation patterns," IET Microwave Antennas Propagation, December 2007, Volume 1, Issue 6, p.1160–1169

[17] 3GPP TSG-RAN WG4, Tdoc R4-093095, Agilent Technologies, "Experimental validation of two-stage MIMO OTA method versus SCM approximation method," ShenZhen, China, August 24–28, August 2009